Linear Dynamics and Stability Analysis of a Two-Craft Coulomb Tether Formation

Arun Natarajan* and Hanspeter Schaub†
Virginia Polytechnic Institute and State University, Blacksburg, Virginia 24061

The linearized dynamics and stability of a two-craft Coulomb tether formation is investigated. With a Coulomb tether the relative distance between two satellites is controlled using electrostatic Coulomb forces. A charge feedback law is introduced to stabilize the relative distance between the satellites to a constant value. Compared to previous Coulomb thrusting research, this is the first feedback control law that stabilizes a particular formation shape. The two craft are connected by an electrostatic tether that is capable of both tensile and compressive forces. As a result, the two-craft formation will essentially act as a long, slender near-rigid body. Interspacecraft Coulomb forces cannot influence the inertial angular momentum of this formation. However, the differential gravitational attraction can be exploited to stabilize the attitude of this Coulomb tether formation about an orbit nadir direction. Stabilizing the separation distance will also stabilize the in-plane rotation angle, whereas the out-of-plane rotational motion remains unaffected. The Coulomb tether has been modeled as a massless, elastic component. The elastic strength of this connection is controlled through a spacecraft charge control law.

I. Introduction

THE concept of formation flying using electrostatic propulsion was introduced in Refs. 1 and 2.‡ The electrostatic (Coulomb) charge of spacecraft is varied by active emission of either negative electric charges (electrons) or positive electric charges (ions). The resulting changes in interspacecraft Coulomb forces are used to control the relative motion of the spacecraft. This novel concept of propellantless relative navigation control has many advantages over conventional thrusters like ion engines. For example, this method of propulsion has been shown to require essentially no consumables (fuel efficiencies ranging up to 10^{13} s), require very little electric power to operate (often less than 1 W), and can be controlled with a very high bandwidth (zero to maximum charge transition times are of the order of milliseconds). Thus, this propulsion concept could enable high-precision formation flying with separation distances ranging between 10–100 m. It is also a very clean method of propulsion compared to ion engines, thereby avoiding the thruster plume contamination issue with neighboring satellites. For this range of separation distances, the plume-impingement problem of high-efficiency ion engines would be severe. Proposed uses of the Coulomb propulsion concept include high-accuracy, wide-field-of-view optical interferometry missions with geostationary orbits (GEO),† controlling clusters of spacecraft to maintain a bounded shape,[2] as well as the use of drone-worker concepts where dedicated craft place a sensor in space using Coulomb forces.[3] A new application of the Coulomb propulsion concept is to use the electrostatic force to control the separation distance between two physically unconnected craft. Because of the similarities with using a tether cable to connect two craft, this concept is called a Coulomb tether formation. Note that contrary to traditional tethers, the Coulomb tether is capable of receiving both tensile and compressive forces. Further, the stiffness of the satellite connection can be controlled through feedback control laws. This will allow for the Coulomb tether stiffness to be varied

with changing mission requirements. Scenarios with two spacecraft flying only dozens of meters apart are investigated. Potential applications include releasing a sensor or camera unit from the primary spacecraft and holding it at fixed distance above or below the spacecraft. From this non-Keplerian orbit, the sensor craft could monitor the spacecraft itself or perform other scientific measurements.

Although the Coulomb propulsion concept has many exciting advantages, it does come at the price of greatly increased coupling and nonlinearity of the charged spacecraft equations of motion. The relative motion of all other neighboring charged craft will be affected by changing the charge of a single craft. Further, with the Coulomb forces being formation-internal forces, some constraints are applicable to all feasible charged spacecraft motion. In particular, Coulomb forces cannot be used to change the total inertial formation angular momentum vector.[4] As a result, these spacecraft charges cannot be used to reorient a formation as a whole to a new orientation. An external influence must be used or generated through thrusters to reorient a Coulomb formation.

When charging spacecraft to control relative motion, differential charging across the spacecraft components must be minimized to avoid arcing. The very simple Coulomb craft used in this study are assumed to be designed to carry a higher Coulomb charge level. However, note that the control charge levels proposed for the Coulomb tether formation are similar to the naturally occurring charge levels of GEO spacecraft during periods of high solar activity. The technology to control the charge involves high-speed ion and electron emitters and is similar to what is currently flying on the CLUSTERS mission[5] or to what flew on the SCATHA mission.[6] On the CLUSTERS mission the spacecraft charge is actively controlled to neutralize its potential relative to the space plasma environment. Because of the high fuel efficiency of the Coulomb thrusting concept,[1,†] where relative motion I_{sp} values can range between 10^{10}–10^{13} s, the change in momentum and plasma environment as a result of the expelled charges is negligible.

Spacecraft are not subjected to the same gravitational pull throughout the body. The sections that are closer to the Earth are attracted more strongly than those that are further away. This force or gravity gradient[7] has been used in stabilizing some satellites. To guarantee linear stability of rigid-body attitudes in orbit, the principal inertias of the body must satisfy well-known constraints. Typically gravity-gradient stabilized satellites are tall and slender and aligned with the local nadir direction. The same concept of stabilization can be extended to the two spacecraft Coulomb tether concept, where the craft are assumed to be flying apart by a few dozen meters. A charge feedback law is employed to stabilize the spacecraft separation distance (making the formation act as a rigid,

---

*Graduate Student, Aerospace and Ocean Engineering Department. Student Member AIAA.
†Assistant Professor, Aerospace and Ocean Engineering Department. Senior Member AIAA.
‡Data available online at http://www.niac.usra.edu [cited Jan. 2002].

slender rod), while the gravity-gradient torque is exploited to assist in stabilizing the formation attitude.

The study of electrostatic charging data of SCATHA spacecraft[6] in GEO has shown that the spacecraft can naturally charge to very high voltages in low plasma environments such as at GEO. The level of natural charge depends on the current solar activity. Further, this mission demonstrated that the spacecraft charge could be actively controlled. The Coulomb propulsion has its own set of limitations, however. The magnitude of Coulomb electrostatic force is inversely proportional to the square of separation distance, which makes this method effective only for close formations of the order of 10–100 m, depending on the maximum allowable level of spacecraft charge. Moreover, if charged plasma particles are present in the space, the effectiveness of Coulomb force is diminished with the electric field dropping off exponentially. The severity of this drop is measured using the Debye length.[8,9] For low Earth orbits (LEO), the Debye length is of the order of centimeters, making the Coulomb formation-flying concept impractical. At geostationary orbits or higher, where the plasma environment is milder, the Debye length is about 100–1400 m. The Coulomb formation-flying concepts can be comfortably applied at this altitude. King et al.[1] found analytical solutions for Hill-frame invariant Coulomb formations. Here spacecraft are placed at specific locations in the rotating Hill frame with specific electrostatic charges. As a result, the Coulomb forces perfectly cancel all natural orbital accelerations, causing the satellites to remain fixed or static as seen by the Hill frame. However, the charge was held constant in their analysis. The discovered open-loop static Coulomb formations were all found to be unstable.

References 1 and 2 discuss the static Coulomb satellite formations and the associated equilibrium charges, but do not address the stabilization of these formations. In this paper, stabilization of a simple static Coulomb structure is discussed for the first time. An active charge feedback control is presented to stabilize the static two-craft formation shape and orientation. To achieve this goal, we use known stability characteristics of orbital rigid-body motion under a gravity-gradient field and examine its applicability to a Coulomb tethered two-spacecraft system. To avoid the very small plasma Debye lengths found at LEO, the Coulomb tether formation studied is at GEO. The formation center of mass or chief motion is assumed to be circular. In formation flying the chief is the reference location about which all other deputy satellites are flying. The two-body Coulomb tether problem considered here can be viewed as a subproblem of the multisatellite formation-flying problem. In future work, attempts will be made to extend the feedback control discussed here to multi-satellite formations. The paper is organized as follows. After discussing the charged spacecraft equations of motion, the equations are rewritten using spherical coordinates and linearized for small departure angles relative to an equilibrium attitude. A feedback charge control law is introduced to stabilize the separation distance, followed by a combined attitude and separation distance linear stability analysis. A numerical simulation illustrates the results and compares the linearized performance predictions to the actual nonlinear system response.

II. Static (Rigid) Formation Dynamics

To start with, the equations of motion of a cluster of charged spacecraft are briefly reviewed. The Clohessy–Wiltshire–Hill's (CW) equations[10,11] are commonly used for spacecraft formation studies. These equations express the linearized motion of one satellite relative to a circularly orbiting reference point or chief location. Note that this chief location does not have to be actually occupied by a satellite. For the present discussion, the formation chief location is set to be equal to the formation center of mass. The various satellites in a formation are called the deputy satellites. The system of Cartesian coordinates used to describe the relative motion of a satellite with respect to the chief location is defined in the rotating Hill orbit frame $\mathcal{O}: \{\hat{o}_r, \hat{o}_\theta, \hat{o}_h\}$ as shown in Fig. 1. The origin of the coordinate system is chosen to be the formation center of mass or chief location. The Cartesian x, y, and z coordinates are the vector
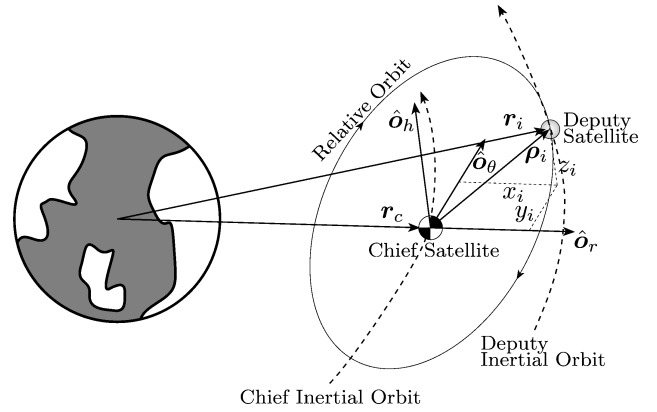

Fig. 1 Rotating hill coordinate system used to describe the relative position of the satellites.

components of the relative position vector

$$\boldsymbol{\rho} = \overset{\mathcal{O}}{\begin{pmatrix} x \\ y \\ z \end{pmatrix}} \qquad (1)$$

along the directions of orbit radial $\hat{o}_r$ (outward), the orbital velocity vector $\hat{o}_\theta$, and the normal vector $\hat{o}_h$ with respect to the orbit plane. Assuming that the Coulomb formation contains N satellites, the CW equations of the ith deputy with respect to the chief are expressed as

$$\ddot{x}_i - 2\Omega \dot{y}_i - 3\Omega^2 x_i = \frac{k_c}{m_i} \sum_{j=1}^{N} \frac{(x_i - x_j)}{|\boldsymbol{\rho}_i - \boldsymbol{\rho}_j|^3} q_i q_j e^{-|\rho_i - \rho_j|/\lambda_d} \qquad j \neq i$$
$$(2a)$$

$$\ddot{y}_i + 2\Omega \dot{x}_i = \frac{k_c}{m_i} \sum_{j=1}^{N} \frac{(y_i - y_j)}{|\boldsymbol{\rho}_i - \boldsymbol{\rho}_j|^3} q_i q_j e^{-|\rho_i - \rho_j|/\lambda_d} \qquad j \neq i \quad (2b)$$

$$\ddot{z}_i + \Omega^2 z_i = \frac{k_c}{m_i} \sum_{j=1}^{N} \frac{(z_i - z_j)}{|\boldsymbol{\rho}_i - \boldsymbol{\rho}_j|^3} q_i q_j e^{-|\rho_i - \rho_j|/\lambda_d} \qquad j \neq i \quad (2c)$$

where $\boldsymbol{\rho}_i = (x_i, y_i, z_i)^T$ is the position vector of the ith satellite in Hill frame components, m_i is the satellite mass, and q_i is the satellite charge. The chief position vector $\boldsymbol{r}_c$ is assumed to have a constant orbital rate of $\Omega = \sqrt{(GM_e/r_c^3)}$, where G is the gravity constant and M_e is the Earth's mass. The parameter $k_c = 8.99 \cdot 10^9 \, \mathrm{Nm^2/C^2}$ is the Coulomb's constant, while the parameter λ_d is the Debye length. Because the Coulomb tether formations are assumed to be at GEO where the Debye length is much larger than the typical Coulomb tether length, the Debye length influence is ignored as a higher-order term for the remainder of the paper. Note that these relative equations of motion of a charged spacecraft contain linearized orbital dynamics, while retaining the full nonlinear Coulomb force expression. In fact, it is this very nonlinear Coulomb force term that causes the strong and complex coupling between the spacecraft motions.

The formation geometry of the ideal two-craft Coulomb tether formation is shown in Fig. 2. As will be shown later in this section, there exists a two-craft static Coulomb formation solution where both masses must be aligned equal distances away from the chief along the nadir direction. The ideal separation distance is called L_{ref}. If each craft has a certain charge, then the resulting Coulomb forces will perfectly cancel the linearized orbital accelerations in the Hill frame. As a result, the two craft would each remain aligned in the chief nadir direction and perform non-Keplerian motions. To an external observer, the two physically unconnected craft would appear to both be performing perfectly circular motions, but with a non-Keplerian orbit period for their individual altitudes. The invisible Coulomb tether is applied to get the required interspacecraft force,
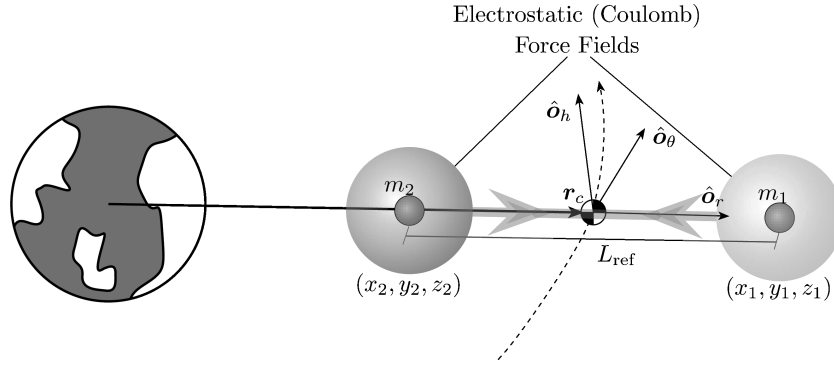
Fig. 2 Coulomb tethered two-satellite formation with the satellites aligned along the orbit nadir direction.

similar to how a cable tether could provide the required tension between the craft to maintain such non-Keplerian orbits.

Because the Coulomb tether formation considered has only two spacecraft, the CW equations in Eq. (2) for satellite 1 can be simplified as

$$\ddot{x}_1 - 2\Omega\dot{y}_1 - 3\Omega^2 x_1 = (k_c/m_1)\big[(x_1 - x_2)\big/L^3\big]q_1q_2 \qquad (3a)$$

$$\ddot{y}_1 + 2\Omega\dot{x}_1 = (k_c/m_1)\big[(y_1 - y_2)\big/L^3\big]q_1q_2 \qquad (3b)$$

$$\ddot{z}_1 + \Omega^2 z_1 = (k_c/m_1)\big[(z_1 - z_2)\big/L^3\big]q_1q_2 \qquad (3c)$$

where L is the distance between the satellites 1 and 2. As the Hill frame $\mathcal{O}$ origin is assumed to be identical to the formation center of mass, the center-of-mass condition dictates that[4]

$$m_1\boldsymbol{\rho}_1 + m_2\boldsymbol{\rho}_2 = 0 \qquad (4)$$

Thus, by controlling the motion of satellite 1 the motion of the second satellite is also determined implicitly through the center-of-mass constraint.

For this top-down spacecraft formation to remain statically fixed relative to the rotating orbit frame $\mathcal{O}$, the CW equations in Eq. (3) must be satisfied with zero initial velocity and acceleration for each vehicle

$$\dot{x}_i = \ddot{x}_i = \dot{y}_i = \ddot{y}_i = \dot{z}_i = \ddot{z}_i = 0$$

For a two-craft Coulomb formation, this is possible if the relative positions are expressed through

$$m_1 x_1 + m_2 x_2 = 0 \qquad (5a)$$

$$x_1 - x_2 = L \qquad (5b)$$

$$x_1 = [m_2/(m_1 + m_2)]L \qquad (5c)$$

$$x_2 = -[m_1/(m_1 + m_2)]L \qquad (5d)$$

$$y_1 = y_2 = z_1 = z_2 = 0 \qquad (5e)$$

Substituting the preceding conditions and constraints in Eq. (3), one obtains the following two spacecraft charge conditions for a static nadir-aligned formation:

$$(k_c/m_1)\big(q_1q_2\big/L^2\big) + 3\Omega^2[m_2L/(m_1 + m_2)] = 0$$

$$\Rightarrow q_1q_2 = -3\Omega^2\big(L^3\big/k_c\big)[m_1m_2/(m_1 + m_2)] \qquad (6a)$$

$$(k_c/m_2)\big(q_1q_2\big/L^2\big) + 3\Omega^2[m_1L/(m_1 + m_2)] = 0$$

$$\Rightarrow q_1q_2 = -3\Omega^2\big(L^3\big/k_c\big)[m_1m_2/(m_1 + m_2)] \qquad (6b)$$

The ideal product of charges Q_{ref} needed to achieve this static Coulomb formation is

$$Q_{\text{ref}} = q_1q_2 = -3\Omega^2\big(L^3\big/k_c\big)[m_1m_2/(m_1 + m_2)] \qquad (7)$$

Thus, if the satellites are placed at the locations shown in Eq. (5), and have the charges q_1 and q_2 satisfying Eq. (7), then the satellites will appear to be frozen or fixed as seen by the rotating frame $\mathcal{O}$. Note that this reference charge product term will be negative! This dictates that the spacecraft charges q_1 and q_2 will have opposite charge signs. However, there are an infinite number of charge pairs that satisfy $Q_{\text{ref}} = q_1q_2$. When implementing charge control strategies in this study, the charge magnitudes are set equal. If one craft is capable of higher charge levels, it is possible to have unequal charges as long as their product satisfies the required $Q = q_1q_2$ value.

III. Linearized Orbital Perturbation

The constant charge computed in accordance with Eq. (7) will only result in the static nadir formation if there are no position or velocity errors and no perturbations are present. Otherwise, the relative separation will become unstable, and the satellites will separate. This problem can be overcome by allowing a suitable variation of charges. In this section, a relationship between these position and charge states is established by considering small perturbations about the established reference states.

Let the two-craft formation be treated as if it were a rigid body. Accordingly, consider a body-fixed coordinate frame $\mathcal{B}$: $\{\hat{\boldsymbol{b}}_1, \hat{\boldsymbol{b}}_2, \hat{\boldsymbol{b}}_3\}$, where $\hat{\boldsymbol{b}}_1$ is aligned with the relative position vector $\boldsymbol{\rho}_1$. Note that if the body is at the ideal Coulomb tether orientation where the masses are aligned exactly along the orbit nadir direction $\hat{\boldsymbol{o}}_r$, then the $\mathcal{O}$ and $\mathcal{B}$ frame orientation vectors are identical. The relative position vector of mass m_1 in body-fixed axes is given by

$$\boldsymbol{\rho}_1 = [m_2/(m_1 + m_2)]L\hat{\boldsymbol{b}}_1 + 0\hat{\boldsymbol{b}}_2 + 0\hat{\boldsymbol{b}}_3 \qquad (8)$$

Let the 3-2-1 Euler angles (ψ, θ, ϕ) represent the Coulomb tether $\mathcal{B}$ frame attitude relative to the orbit frame $\mathcal{O}$ for small angular perturbations as shown in Fig. 3. Because point masses are being considered, the rotation about $\hat{\boldsymbol{b}}_1$ (angle ϕ) can be neglected. The direction cosine matrix $[BO(\psi, \theta)]$, which relates the $\mathcal{O}$ frame to $\mathcal{B}$ frame, is given by

$$[BO] = \begin{bmatrix} \cos\theta\cos\psi & \cos\theta\sin\psi & -\sin\theta \\ -\sin\psi & \cos\psi & 0 \\ \sin\theta\cos\psi & \sin\theta\sin\psi & \cos\theta \end{bmatrix} \qquad (9)$$

Using small angle approximations for the trigonometric functions, the position vector of mass m_1 in $\mathcal{O}$ frame can be written as

$$\begin{pmatrix} x_1 \\ y_1 \\ z_1 \end{pmatrix} = [BO]^T \begin{pmatrix} [m_2/(m_1 + m_2)]L \\ 0 \\ 0 \end{pmatrix}$$

$$\approx \begin{pmatrix} [m_2/(m_1 + m_2)]L \\ \psi[m_2/(m_1 + m_2)]L \\ -\theta[m_2/(m_1 + m_2)]L \end{pmatrix} \qquad (10)$$
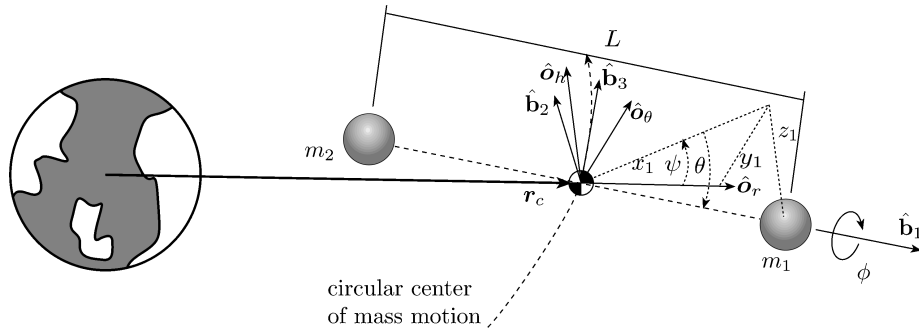
Fig. 3   Euler angles representing the attitude of Coulomb tether with respect to the orbit frame.

Taking the derivative of this expression, the linearized Hill frame relative velocity coordinates are found to be

$$\begin{pmatrix} \dot{x}_1 \\ \dot{y}_1 \\ \dot{z}_1 \end{pmatrix} \approx \frac{m_2}{m_1 + m_2} \begin{pmatrix} \dot{L} \\ \psi \dot{L} + \dot{\psi} L \\ -\theta \dot{L} - \dot{\theta} L \end{pmatrix} \qquad (11)$$

The distance L between the two masses m_1 and m_2 is given by

$$L^2 = (x_1 - x_2)^2 + (y_1 - y_2)^2 + (z_1 - z_2)^2 \qquad (12)$$

Using the center-of-mass condition in Eq. (4), this can be simplified to

$$L^2 = [(m_1 + m_2)/m_2]^2 (x_1^2 + y_1^2 + z_1^2) \qquad (13)$$

Differentiating Eq. (4) twice and substituting Eq. (3) into the resulting expression yields

$$\dot{L}^2 + L\ddot{L} = [(m_1 + m_2)/m_2]^2 \Big(\dot{x}_1^2 + x_1 \{ 2\Omega \dot{y}_1 + 3\Omega^2 x_1 $$
$$+ (k_c/m_1)[(x_1 - x_2)/L^3]Q \} + \dot{y}_1^2 $$
$$+ y_1 \{ -2\Omega \dot{x}_1 + (k_c/m_1)[(y_1 - y_2)/L^3]Q \} $$
$$+ \dot{z}_1^2 + z_1 \{ -\Omega^2 z_1 + (k_c/m_1)[(z_1 - z_2)/L^3]Q \} \Big) \qquad (14)$$

Transforming the Cartesian coordinates (x_1, y_1, z_1) to spherical coordinates (L, ψ, θ) using Eqs. (10) and (11), while neglecting higher-order terms in ψ and θ, we get the linearized differential equation of the separation distance L:

$$\ddot{L} = (2\Omega\dot{\psi} + 3\Omega^2)L + (k_c/m_1)Q(1/L^2)[(m_1 + m_2)/m_2] \quad (15)$$

Note the following special case. Assume that the charge product term Q is zero (i.e., classical Keplerian motion) and that the satellites are initially at rest with $\dot{\psi} = 0$. In this case the separation distance equations of motion simplify to

$$\ddot{L} - 3\Omega^2 L = 0$$

This unstable oscillator equation demonstrates that without any Coulomb force active this formation could not remain at the specific nadir locations.

Next the separation distance equations of motion are linearized about small variations in length δL and small variations in the product charge term δQ. The reference separation length L_{ref} is determined by the mission requirement. The reference charge product term is determined through the L_{ref} choice and the constraint in Eq. (7).

$$L = L_{\text{ref}} + \delta L \qquad (16a)$$

$$Q = Q_{\text{ref}} + \delta Q \qquad (16b)$$

Substituting these L and Q definitions into Eq. (15) and linearizing leads to

$$\delta\ddot{L} = (2\Omega L_{\text{ref}})\dot{\psi} + (9\Omega^2)\delta L + \big\{ (k_c/m_1)\big(1/L_{\text{ref}}^2\big) $$
$$\times [(m_1 + m_2)/m_2] \big\} \delta Q \qquad (17)$$

This equation establishes the desired relationship between the additional charge product δQ required and the change in relative separation of the satellites. It is observed that this relation is coupled to the body-frame yaw rate $\dot{\psi}$. The Coulomb tether attitude differential equations will be developed later using angular momentum expressions.

To develop a feedback law to control the separation distance using the Coulomb forces, the small charge product variation δQ is treated as a control variable. Because the charge of each craft causes a force along the relative position vector, the Coulomb charges can be used to control the spacecraft separation distance. By defining

$$\delta Q = \frac{m_1 m_2 L_{\text{ref}}^2}{(m_1 + m_2)k_c}(-C_1 \delta L - C_2 \delta \dot{L}) \qquad (18)$$

the closed-loop separation distance dynamics become

$$\delta\ddot{L} + \big(C_1 - 9\Omega^2\big)\delta L + C_2 \delta\dot{L} - (2\Omega L_{\text{ref}})\dot{\psi} = 0 \qquad (19)$$

This control law provides both proportional and derivative feedback of δL. Because the δL differential equation does not contain a damping term $\delta\dot{L}$, the inclusion of the derivative feedback is essential to ensure asymptotic convergence. Note that in the absence of the yaw rate term $\dot{\psi}$, these closed-loop dynamics would be stable if $C_1 > 9\Omega^2$ and $C_2 > 0$. However, because of the coupling with the yaw (in-orbit-plane) rotation the complete Coulomb tether motion must be analyzed for stability.

To implement this charge feedback control law, the spacecraft charges q_1 and q_2 must be determined. The value of Q_{ref} is determined through Eq. (7), while the value of δQ is given by the feedback law expression in Eq. (18). Thus, the spacecraft charges q_1 and q_2 must satisfy

$$q_1 q_2 = Q_{\text{ref}} + \delta Q \qquad (20)$$

There are an infinite number of solutions to the preceding constraint. To keep the charges equal in magnitude across the craft, the following implementation was used:

$$q_1 = \sqrt{|Q_{\text{ref}} + \delta Q|} \qquad (21)$$

$$q_2 = -q_1 \qquad (22)$$

Note that here $Q_{\text{ref}} + \delta Q < 0$ because $\delta Q \ll Q_{\text{ref}}$ and $Q_{\text{ref}} < 0$. With this charging convention we find $q_1 > 0$ and $q_2 < 0$.

IV. Stability Analysis Using Gravity Gradient

In this section the stability of both the Coulomb tether attitude (ψ, θ) and the separation distance L is analyzed. The gravity-gradient torque is included to exert an external torque onto the Coulomb tether. Let the orbit angular velocity vector relative to the inertial frame $\mathcal{N}$ be given by

$$\boldsymbol{\omega}_{\mathcal{O}/\mathcal{N}} = \Omega \hat{o}_h \tag{23}$$

To develop the tether attitude differential equations of motion, the two-craft formation is treated as a continuous body. This is motivated by the stable Coulomb tether formation acting as a rigid dumbbell spacecraft. The formation inertia matrix is expressed as[7]

$$[I] = -m_1[\tilde{\rho}_1][\tilde{\rho}_1] - m_2[\tilde{\rho}_2][\tilde{\rho}_2] \tag{24}$$

where $[\tilde{\rho}_1]$ is a skew-symmetric matrix, which is equivalent to the vector cross-product operator $\boldsymbol{a} \times \boldsymbol{b} \simeq [\tilde{a}]\boldsymbol{b}$. For the two-craft Coulomb tether formation, using the center-of-mass definition in Eq. (4), the inertia matrix is trivially given in the body frame $\mathcal{B}$ as

$$^{\mathcal{B}}[I] = \begin{bmatrix} 0 & 0 & 0 \\ 0 & I & 0 \\ 0 & 0 & I \end{bmatrix} \tag{25}$$

where

$$I = [m_1 m_2/(m_1 + m_2)]L^2 \tag{26}$$

Note that these moments of inertia vary with time because of their dependence on the variable formation length L. The $\mathcal{B}$-frame derivative of the inertia matrix is

$$^{\mathcal{B}}[\dot{I}] = \begin{bmatrix} 0 & 0 & 0 \\ 0 & \dot{I} & 0 \\ 0 & 0 & \dot{I} \end{bmatrix} \tag{27}$$

where

$$\dot{I} = 2[m_1 m_2/(m_1 + m_2)]L\dot{L}$$
$$= 2[m_1 m_2/(m_1 + m_2)](L_{\text{ref}} + \delta L)\delta\dot{L} \tag{28}$$

because $L_{\text{ref}} = $ constant.

To develop the attitude differential equations, the total inertial angular momentum of the two-craft formation is

$$\boldsymbol{H} = [I](\boldsymbol{\omega}_{\mathcal{B}/\mathcal{O}} + \boldsymbol{\omega}_{\mathcal{O}/\mathcal{N}}) \tag{29}$$

Because the Coulomb control forces are all formation internal forces, one finds that the inertial derivative of $\boldsymbol{H}$ is equal to the total external torque acting on the system. Euler's rotational equation of motion with a time-varying inertia matrix $[I]$ and gravity-gradient torque vector $\boldsymbol{L}_G$ is given in body-frame $\mathcal{B}$ components by

$$^{\mathcal{B}}[I]\,^{\mathcal{B}}\dot{\boldsymbol{\omega}} + ^{\mathcal{B}}[\dot{I}]\,^{\mathcal{B}}\boldsymbol{\omega} + ^{\mathcal{B}}[\tilde{\omega}]\,^{\mathcal{B}}[I]\,^{\mathcal{B}}\boldsymbol{\omega} = ^{\mathcal{B}}\boldsymbol{L}_G \tag{30}$$

where $^{\mathcal{B}}\boldsymbol{\omega} = ^{\mathcal{B}}\boldsymbol{\omega}_{\mathcal{B}/\mathcal{N}}$ and the notation $[\tilde{\omega}]\boldsymbol{x} \equiv \boldsymbol{\omega} \times \boldsymbol{x}$ is used. Using the direction cosine matrix definition in Eq. (9), the orbit angular velocity vector can be written as

$$^{\mathcal{B}}\boldsymbol{\omega}_{\mathcal{O}/\mathcal{N}} = [BO]\,^{\mathcal{O}}\boldsymbol{\omega}_{\mathcal{O}/\mathcal{N}} = \begin{bmatrix} -\Omega \sin\theta \\ 0 \\ \Omega \cos\theta \end{bmatrix} \tag{31}$$

The yaw and pitch rates of the Coulomb tether body frame $\mathcal{B}$ relative to the orbit $\mathcal{O}$ frame yield

$$^{\mathcal{B}}\boldsymbol{\omega}_{\mathcal{B}/\mathcal{O}} = \begin{bmatrix} -\sin\theta & 0 \\ 0 & 1 \\ \cos\theta & 0 \end{bmatrix} \begin{bmatrix} \dot{\psi} \\ \dot{\theta} \end{bmatrix} \tag{32}$$

The Coulomb tether body-frame angular velocity vector relative to the inertial frame $\mathcal{N}$ is

$$^{\mathcal{B}}\boldsymbol{\omega}_{\mathcal{B}/\mathcal{N}} = ^{\mathcal{B}}\boldsymbol{\omega}_{\mathcal{B}/\mathcal{O}} + ^{\mathcal{B}}\boldsymbol{\omega}_{\mathcal{O}/\mathcal{N}} = \begin{bmatrix} -\sin\theta\,\dot{\psi} - \Omega\sin\theta \\ \dot{\theta} \\ \cos\theta\,\dot{\psi} + \Omega\cos\theta \end{bmatrix} \tag{33}$$

Linearizing Eq. (33) about small yaw and pitch angles, we get

$$^{\mathcal{B}}\boldsymbol{\omega}_{\mathcal{B}/\mathcal{N}} \approx \begin{bmatrix} -\Omega\theta \\ \dot{\theta} \\ \dot{\psi} + \Omega \end{bmatrix} \tag{34}$$

Taking the inertial derivative of this vector and noting that Ω is constant in this application, the $\mathcal{B}$ frame angular acceleration is

$$^{\mathcal{B}}\dot{\boldsymbol{\omega}}_{\mathcal{B}/\mathcal{N}} \approx \begin{bmatrix} -\Omega\dot{\theta} \\ \ddot{\theta} \\ \ddot{\psi} \end{bmatrix} \tag{35}$$

The gravity-gradient torque $\boldsymbol{L}_G$ also has to be expressed using the tether coordinates. The center-of-mass position vector $\boldsymbol{r}_c$, given in $\mathcal{O}$ frame components as

$$\boldsymbol{r}_c = ^{\mathcal{O}}\begin{pmatrix} r_c \\ 0 \\ 0 \end{pmatrix} \tag{36}$$

is transformed to the $\mathcal{B}$ frame as

$$\boldsymbol{r}_c = ^{\mathcal{B}}\begin{pmatrix} r_{c1} \\ r_{c2} \\ r_{c3} \end{pmatrix} = ^{\mathcal{B}}\begin{pmatrix} \cos\theta\cos\psi \\ -\sin\psi \\ \sin\theta\cos\psi \end{pmatrix} r_c \tag{37}$$

Reference 7 provides the following expression for gravity gradient:

$$^{\mathcal{B}}\begin{bmatrix} L_{G_1} \\ L_{G_2} \\ L_{G_3} \end{bmatrix} = \frac{3GM_e}{r_c^5} \begin{bmatrix} r_{c2}r_{c3}(I_{33} - I_{22}) \\ r_{c1}r_{c3}(I_{11} - I_{33}) \\ r_{c1}r_{c2}(I_{22} - I_{11}) \end{bmatrix} \tag{38}$$

After substituting for r_{c_i} from Eq. (37) and using the known value of Ω from Kepler's equation, namely,

$$GM_e/r_c^3 = \Omega^2 \tag{39}$$

the gravity-gradient torque vector acting on the Coulomb tether body frame is written as

$$^{\mathcal{B}}\boldsymbol{L}_G \cong 3\Omega^2 \begin{bmatrix} 0 \\ -I\theta \\ -I\psi \end{bmatrix} \tag{40}$$

Substituting these results for $\boldsymbol{L}_G$, $^{\mathcal{B}}[\dot{I}]$, $^{\mathcal{B}}[I]$, $\boldsymbol{\omega}_{\mathcal{B}/\mathcal{N}}$ and $\dot{\boldsymbol{\omega}}_{\mathcal{B}/\mathcal{N}}$ back into Euler's rotational equations of motion in Eq. (30), and after simplifying the algebra the resulting linearized attitude dynamics of the Coulomb tether body frame $\mathcal{B}$ are written along with the separation distance differential equation as

$$\ddot{\theta} + 4\Omega^2\theta = 0 \tag{41a}$$

$$\ddot{\psi} + (2\Omega/L_{\text{ref}})\delta\dot{L} + 3\Omega^2\psi = 0 \tag{41b}$$

$$\delta\ddot{L} + C_2\delta\dot{L} - (2\Omega L_{\text{ref}})\dot{\psi} + (C_1 - 9\Omega^2)\delta L = 0 \tag{41c}$$

Thus, Eqs. (41a–41c) are the linearized equations of motion of the Coulomb tether body about that static nadir reference configuration. Only the linearized δL differential equation was obtained using the Clohessy–Wiltshire–Hill equations, whereas the linearized differential equations of ψ and θ were derived from the full formation

angular momentum expression along with Euler's equation. These equations have terms that depend on orbital rate Ω, which happens to be a small value at GEO. To avoid numerical issues while carrying out numerical integrations, it is desired to have these equations be independent of Ω. This can be achieved by using the following transformation:

$$d\tau = \Omega \, dt \tag{42a}$$

$$(*)' = \frac{d(*)}{d\tau} = \frac{1}{\Omega}\frac{d(*)}{dt} \tag{42b}$$

By carrying out the preceding transformation in Eqs. (41a–41c), the orbit rate Ω independent linearized equations of motion of the Coulomb tether body are given by

$$\theta'' + 4\theta = 0 \tag{43a}$$

$$\psi'' + (2/L_{\text{ref}})\delta L' + 3\psi = 0 \tag{43b}$$

$$\delta L'' + \tilde{C}_2 \delta L' - (2L_{\text{ref}})\psi' + (\tilde{C}_1 - 9)\delta L = 0 \tag{43c}$$

where $\tilde{C}_2 = (C_2/\Omega)$ and $\tilde{C}_1 = (C_1/\Omega^2)$ are nondimensionalized feedback gains. It can be observed from these equations that the out-of-plane motion $\theta(t)$ is decoupled and its equation is that of a simple oscillator. This decoupling is analogous to what occurs with the linearized rigid-body attitude dynamics subject to a gravity-gradient torque. Because the $\theta(t)$ motion is not coupled to the tether charge product term δQ or the separation distance variation δL, it is not possible to control the pitch motion θ with the Coulomb charge in this linearized analysis. The yaw motion $\psi(t)$ is coupled with the $\delta L(t)$ motion in the form of a driving force, which might make it amenable to asymptotic stabilization by controlling the charge.

The values of gain $\tilde{C}_1$ and $\tilde{C}_2$ can be tuned to meet the stability requirements using the Routh–Hurwitz stability criterion. The characteristic equation for the coupled δL and ψ equations is

$$\lambda^4 + \tilde{C}_2\lambda^3 + (\tilde{C}_1 - 2)\lambda^2 + 3\tilde{C}_2\lambda + 3(\tilde{C}_1 - 9) = 0 \tag{44}$$

Although the linearized closed-loop dynamics do depend on the Coulomb tether reference length L_{ref}, note that the characteristic equation does not. To ensure asymptotic stability, roots of this equation should have negative real parts. The constraints on the gains $\tilde{C}_1$ and $\tilde{C}_2$ for meeting this condition are identified by constructing a Routh table and are found to be

$$\tilde{C}_1 > 9 \tag{45a}$$

$$\tilde{C}_2 > 0 \tag{45b}$$

Incidentally, these constraints also ensure the stability of δL equation ignoring the ψ' term.

The stability criterion imposes constraints on the choice of the feedback gains $\tilde{C}_1$, $\tilde{C}_2$ but is not enough to actually decide their values. One needs to look for alternate criteria for fixing them. One satisfying way would be to fix the gains by demanding conditions of critical or near critical damping. For ease of discussion, let the feedback gains be expressed in terms of scaling factor n and α, both taken as positive and real. The gains can be rewritten as

$$\tilde{C}_1 = n > 9 \tag{46}$$

and

$$\tilde{C}_2 = \alpha\sqrt{n - 9} \tag{47}$$

The natural frequency of the ψ equation is $\sqrt{3}$ and is not affected by the choice of $\tilde{C}_1$ and $\tilde{C}_2$, whereas the natural frequency for δL equation is $\sqrt{(n - 9)}$. The value of $n = 12$ will match these frequencies making the ψ' coupling term in δL equation serve as de facto damping term. A similar remark applies to the ψ equation. In Eq. (47), $\alpha = 2$ ensures that the δL equation without the ψ' term

Table 1 Input parameters used in simulation

Parameter	Value	Units
m_1	150	kg
m_2	150	kg
L_{ref}	25	m
k_c	8.99×10^9	Nm^2/C^2
Q_{ref}	-2.07911	μC^2
Ω	7.2915×10^{-5}	rad/sec
n	12	
α	2.28	
$\delta L(0)$	0.5	m
$\psi(0)$	0.1	rad
$\theta(0)$	0.1	rad

a) Gain $\alpha = 2.0$
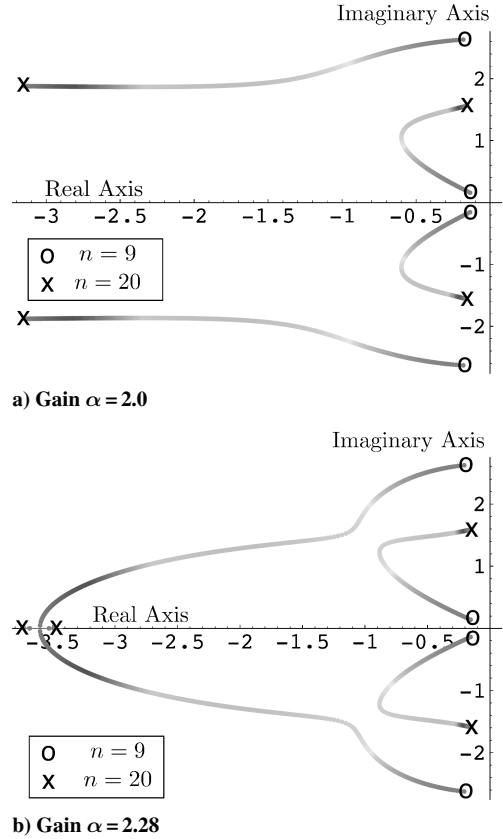

b) Gain $\alpha = 2.28$

Fig. 4 Root-locus plot of the linearized spherical coordinate differential equations for different gain α values.

is critically damped. For effective damping with the inclusion of ψ' term, the value of α and n need to be modified. However, one expects the value of α to be in the vicinity of $\alpha = 2$ and n to be around 12. Hence, root-locus plots for the coupled δL and ψ equations are studied with a range of α values in the vicinity of $\alpha = 2$ with n varying between 9 and 20. Figure 4 shows the root-locus plots for two different α values. Studying the root-locus plots, it can be observed that as the n value increases beyond 12 the rate of convergence of one of the modes increases and the other decreases. Therefore, $n = 12$ is ideal for ensuring good rates of convergence for both of the modes. It is also noted that $\alpha = 2.28$ resulted in effective damping for the modes.

V. Numerical Simulation

A numerical simulation is presented to illustrate the performance and stability of a 25-m Coulomb tether formation. The simulation parameters that were used are listed in Table 1. The initial attitude values are set to $\psi = 0.1$ radians and $\theta = 0.1$ rad. The separation length error (Coulomb tether length error) is $\delta L = 0.5$ m. All initial rates are set to zero through $\dot{\psi} = \delta\dot{L} = \dot{\theta} = 0$.

a) Time histories of length variations δL, in-plane rotation angle ψ, and out-of-plane rotation angle θ
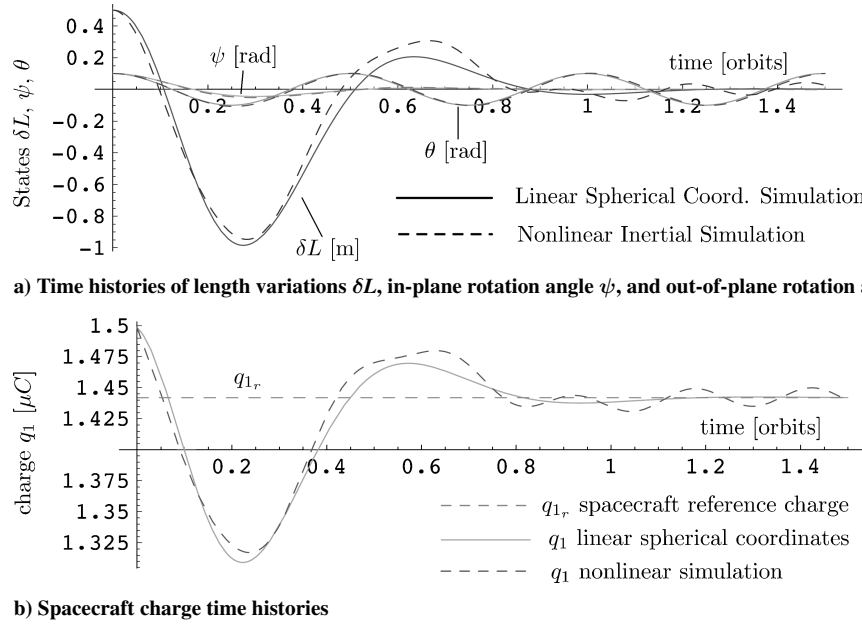

b) Spacecraft charge time histories

Fig. 5 Simulation results of integrating either the linearized spherical coordinates differential equations (——) or the nonlinear inertial coordinate differential equations (- - - -).

The choice of values for the gains $\tilde{C}_1$ and $\tilde{C}_2$ should not only satisfy the stability criterion mentioned in Eq. (45) but also should be such as to lead to near-ideal damping. Studying the root-locus plots where the parameters n and α are varied, the values $n = 12$ and $\alpha = 2.28$ were chosen. Hence, using Eq. (47) the gain $\tilde{C}_2$ was found to be $2.28\sqrt{3}$.

The Coulomb tether performance was simulated in two different manner. First the linearized spherical coordinate differential equations were integrated. This simulation illustrates the linear performance of the charge control. Second, the linearized results were compared with those obtained from the exact nonlinear equation of motion of the deputy satellites given by

$$\ddot{\boldsymbol{r}}_1 + \left(\mu/r_1^3\right)\boldsymbol{r}_1 = (k_c/m_1)(Q/L^3)(\boldsymbol{r}_1 - \boldsymbol{r}_2) \qquad (48a)$$

$$\ddot{\boldsymbol{r}}_2 + \left(\mu/r_2^3\right)\boldsymbol{r}_2 = (k_c/m_2)(Q/L^3)(\boldsymbol{r}_2 - \boldsymbol{r}_1) \qquad (48b)$$

where $\boldsymbol{r}_1 = \boldsymbol{r}_c + \boldsymbol{\rho}_1$ and $\boldsymbol{r}_2 = \boldsymbol{r}_c + \boldsymbol{\rho}_2$ are the inertial position vectors of the the masses m_1 and m_2, while $L = \sqrt{[(\boldsymbol{r}_2 - \boldsymbol{r}_1) \cdot (\boldsymbol{r}_2 - \boldsymbol{r}_1)]}$. The gravitational coefficient μ is defined as $\mu \approx GM_e$. After integrating the motion using inertial Cartesian coordinates, the separation distance L, as well as the in-plane and out-of-plane angles ψ and θ, are computed in postprocessing using the exact kinematic transformation. The Debye length is kept at zero during this simulation to study in detail the effects of the relative motion linearization.

Figure 5a shows the Coulomb tether motion in the linearized spherical coordinates (ψ, θ, δL), along with the full nonlinear spherical coordinates shown as dashed lines. With the presented charge feedback law, both the yaw motion ψ and the separation distance deviation δL converged to zero. By stabilizing the δL state to zero, the in-plane rotation $\psi(t)$ also converges to zero. For the set of initial conditions used in this simulation, the δL and ψ states have converged after about 0.9 orbits. As expected, the pitch motion $\theta(t)$ was a stable sinusoidal motion. Further, Fig. 5a shows that the nonlinear simulation closely follows the linearized simulation. However, there is one notable difference. The δL states converge to zero asymptotically in the linearized simulation, while they achieve a steady-state oscillation in the nonlinear simulation. This difference in behavior occurs because the same reference charge product Q_{ref} [computed using Eq. (7)] is used in both simulations. This charge will achieve a static formation in the linearized CW equations. However, this charge value will not achieve a static formation in the nonlinear problem. Thus, the charge feedback control is not actually oper-

ating about a proper steady-state charge of the nonlinear problem. As the δL and ψ tracking errors go to zero, the orbital dynamics will perturb the system and cause these states to grow again. This persistent disturbance results in the final steady-state oscillations shown. To implement such a control strategy for an actual mission, the Q_{ref} value would be recomputed numerically for the nonlinear problem. Even with this deviation, the nonlinear and linear performance predictions compare very well, thus verifying the presented linearization results.

Figure 5b shows the spacecraft control charge q_1 for both the linearized and full nonlinear simulation models. Both are converging to the reference value pertaining to the static equilibrium. As defined, the control charge q_2 is just the negative of q_1. Note that the deviation from the value of reference charges is small, justifying the linearization assumptions used. The magnitude of the control charges is in the order of micro-Coulomb, which is easily realizable in practice using charge emission devices.

VI. Conclusions

The concept of a Coulomb (electrostatic) tether is introduced to bind two satellites in a near-rigid formation. Although the Coulomb force cannot directly stabilize the attitude, the gravity-gradient torque is exploited to stabilize the Coulomb tether formation about the orbit radial direction. The formulation allows for unequal masses. The analysis is based on a linearized dynamics and charge behavior model whose validity is also shown. It was observed that a linear charge feedback law in terms of separation distance errors and separation rate is adequate for stabilizing the separation distance and in-plane angular motion. The control charges needed are small in the order of micro-Coulombs and realizable in practice.

References

[1]King, L. B., Parker, G. G., Deshmukh, S., and Chong, J.-H., "Study of Interspacecraft Coulomb Forces and Implications for Formation Flying," *Journal of Propulsion and Power*, Vol. 19, No. 3, 2003, pp. 497–505.

[2]Schaub, H., Parker, G. G., and King, L. B., "Challenges and Prospect of Coulomb Formations," American Astronautical Society, Paper AAS-03-278, May 2003.

[3]Parker, G. G., Passerello, C. E., and Schaub, H., "Static Formation Control Using Interspacecraft Coulomb Forces," 2nd International Symposium on Formation Flying Missions and Technologies, NASA, Washington DC, Sept. 2004.

[4]Schaub, H., and Kim, M., "Orbit Element Difference Constraints for Coulomb Satellite Formations," AIAA Paper 04-5213, Aug. 2004.

[5]Torkar, K., Riedler, W., Escoubet, C. P., Fehringer, M., Schmidt, R., Grard, R. J. L., Arends, H., Rüdenauer, F., Steiger, W., Narheim, B. T., Svenes, K., Torbert, R., André, M., Fazakerley, A., Goldstein, R., Olsen, R. C., Pedersen, A., Whipple, E., and Zhao, H., "Active Spacecraft Potential Control for Cluster—Implementation and First Results," *Annales Geophysicae*, Vol. 19, Oct. 2001, pp. 1289–1302.

[6]Mullen, E. G., Gussenhoven, M. S., Hardy, D. A., Aggson, T. A., Ledley, B. G., and Whipple, E., "SCATHA Survey of High-Level Spacecraft Charging in Sunlight," *Journal of the Geophysical Research*, Vol. 91, 1986, pp. 1474–1490.

[7]Schaub, H., and Junkins, J. L., *Analytical Mechanics of Space Systems*, AIAA Education Series, AIAA Reston, VA, 2003, pp. 160–171.

[8]Nicholson, D. R., *Introduction to Plasma Theory*, Krieger, Malabar, FL, 1992, pp. 1–3.

[9]Gombosi, T. I., *Physics of the Space Environment*, Cambridge Univ. Press, Cambridge, U.K., 1998, pp. 56–58.

[10]Clohessy, W. H., and Wiltshire, R. S., "Terminal Guidance System for Satellite Rendezvous," *Journal of the Aerospace Sciences*, Vol. 27, No. 9, 1960, pp. 653–658.

[11]Hill, G. W., "Researches in the Lunar Theory," *American Journal of Mathematics*, Vol. 1, No. 1, 1878, pp. 5–26.